# *t-J* model of coupled $Cu_2O_5$ ladders in $Sr_{14-x}Ca_xCu_{24}O_{41}$

Krzysztof Wohlfeld,[1,2] Andrzej M. Oleś,[2,3] and George A. Sawatzky[4]
[1]*IFW Dresden, P.O. Box 270116, D-01171 Dresden, Germany*
[2]*Marian Smoluchowski Institute of Physics, Jagellonian University, Reymonta 4, PL-30059 Kraków, Poland*
[3]*Max-Planck-Institut für Festkörperforschung, Heisenbergstrasse 1, D-70569 Stuttgart, Germany*
[4]*Department of Physics and Astronomy, University of British Columbia, Vancouver, British Columbia, Canada V6T-1Z1*
(Received 11 November 2009; revised manuscript received 4 June 2010; published 24 June 2010)

Starting from the proper charge-transfer model for $Cu_2O_5$ coupled ladders in $Sr_{14-x}Ca_xCu_{24}O_{41}$ we derive the low-energy Hamiltonian for this system. It occurs that the widely used ladder *t-J* model is not sufficient and has to be supplemented by the Coulomb-repulsion term between holes in the neighboring ladders. Furthermore, we show how a simple mean-field solution of the derived *t-J* model may explain the onset of the charge-density wave with the odd period in $Sr_{14-x}Ca_xCu_{24}O_{41}$.

DOI: 10.1103/PhysRevB.81.214522 PACS number(s): 74.72.−h, 71.10.Fd, 71.45.Lr, 75.10.Lp

## I. INTRODUCTION

It is widely assumed that the two-dimensional (2D) *t-J* model[1] is *the* correct model to describe the low-energy physics of the $CuO_2$ planes.[2,3] Consequently, many authors believe that the high-temperature superconductivity in the cuprates *can be* explained by this model and it is merely the computationally challenging character of the model which leads to the lack of the understanding of the superconducting ground state (see, e.g., Ref. 4).

Similarly, it has been suggested that the *t-J* model defined on the ladder (called ladder *t-J* model in what follows) is the right model to describe the low-energy physics relevant for the $Cu_2O_5$ coupled ladder planes of $Sr_{14-x}Ca_xCu_{24}O_{41}$ (SCCO).[5,6] This is a very attractive theoretical idea because: (i) the ladder *t-J* model is much easier to solve than its 2D counterpart and it has a superconducting ground state for some specific range of parameters,[7] (ii) a superconducting ground state (under pressure of 3 GPa) was found[8] in the ladder planes of SCCO for $x=13.6$. This may suggest that indeed the *t-J* model contains the essential physics needed to explain the superconductivity, at least in the ladders.

In this paper we would like to question the above point of view. As we show below, the ladder *t-J* model is too oversimplified and thus, not sufficient to describe the low-energy physics of the ladder planes in SCCO. Actually, this can already be inferred by comparing the experimental observations in SCCO with the theoretical predictions for the ladders:[9] (i) a charge-density wave (CDW) ground state with periods 3 and 5 was observed but (ii) no CDW state with even period has been found,[6] whereas (iii) the ladder *t-J* model may have a CDW ground state only with an even period.[10,11] Therefore, we investigate this problem here by a systematic derivation of the proper *t-J* model for the coupled ladder system, extended primarily for topological reasons by the interladder repulsive term, and discuss a simple solution of this model.

The paper is organized as follows. We introduce the charge-transfer Hamiltonian in Sec. II. Next, in Sec. III we derive the low-energy *t-J* Hamiltonian which contains the kinetic energy and the superexchange, similar to the ladder *t-J* model, and the intraladder and interladder repulsion terms. In Sec. IV we examine the role of the Coulomb intersite repulsion. Finally, we present a numerical solution of the model in Sec. V and draw conclusions in Sec. VI. The paper is supplemented by two appendices where some of the mathematical details of the model derivation are discussed.

## II. CHARGE-TRANSFER HAMILTONIAN

As the starting point we choose the multiband charge-transfer Hamiltonian introduced before for the $Cu_2O_5$ coupled-ladder geometry in SCCO.[9] The model in hole notation reads

$$\mathcal{H} = \mathcal{H}_0 + \mathcal{H}_1 + \mathcal{H}_2, \tag{1}$$

$$\mathcal{H}_0 = -t_{pd}\sum_{i\alpha\sigma}(d^\dagger_{i\alpha\sigma}y_{i\alpha\sigma} - d^\dagger_{i+1,\alpha\sigma}y_{i\alpha\sigma} \mp d^\dagger_{i\alpha\sigma}x_{i\alpha\sigma} \pm d^\dagger_{i\alpha\sigma}b_{i\sigma} + \text{H.c.}) + \Delta\sum_{i\alpha}(n_{i\alpha x}+n_{i\alpha y}) + \Delta\sum_i n_{ib} + U\sum_{i\alpha} n_{i\alpha\uparrow}n_{i\alpha\downarrow}, \tag{2}$$

$$\mathcal{H}_1 = U_p\sum_{i\alpha,\xi=x,y} n_{i\alpha\xi\uparrow}n_{i\alpha\xi\downarrow} + U_p\sum_i n_{ib\uparrow}n_{ib\downarrow}, \tag{3}$$

$$\mathcal{H}_2 = U_p(1-2\eta)\sum_{i\alpha\sigma}(n_{i\alpha x\sigma}\bar{n}_{i\bar{\alpha}y\bar{\sigma}} + n_{i\alpha y\sigma}\bar{n}_{i\bar{\alpha}x\bar{\sigma}}) + U_p(1-3\eta)\sum_{i\alpha\sigma}(n_{i\alpha x\sigma}\bar{n}_{i\bar{\alpha}y\sigma} + n_{i\alpha y\sigma}\bar{n}_{i\bar{\alpha}x\sigma}). \tag{4}$$

The model [Eq. (1)] was adopted to the present ladder geometry[9] from the charge-transfer models introduced before for $CuO_2$ planes,[12] and $CuO_3$ chains[13] in high-temperature superconductors. The parameters are: the energy for oxygen $2p_\sigma$ ($2p_x$ or $2p_y$ with creation operators $\{x^\dagger_{i\alpha\sigma}\}$ and $\{y^\dagger_{i\alpha\sigma}\}$) orbital $\Delta$ (the so-called charge-transfer energy measured with respect to the energy of $3d$ copper orbitals), the *d-p* hopping $t_{pd}$ between the nearest-neighbor copper and oxygen sites, the on-site Coulomb repulsion $U$ ($U_p$) on the copper (oxygen) sites, and $\eta=J_H/U_p\simeq 0.2$—a realistic value of Hund's exchange on oxygen ions[14] (for a complete set of realistic

 

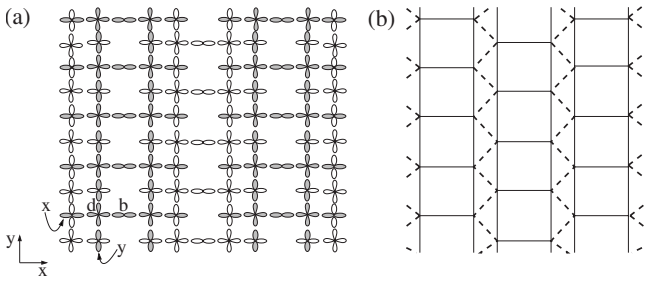


FIG. 1. Schematic view of the coupled $Cu_2O_5$ (white/gray) ladders in SCCO: (a) orbitals in charge-transfer model [Eq. (1)]; (b) intraladder (interladder) bonds in the effective extended *t-J* model, see Eq. (5), shown by solid (dashed) lines.

parameters see Sec. III E). Besides, in principle the actual electron energy at bridge orbital (rung position) of the ladder with creation operators $\{b^\dagger_{i\sigma}\}$ is approximately 10% smaller than the one at other oxygen positions.[15] However, it was shown[16] that this difference does not have any important physical consequences and therefore we will neglect it here. Note also that the phases of the $\{3d,2p\}$ orbitals were explicitly taken into account in the hopping elements $\propto t_{pd}$ (for clarity the phases are shown only in Fig. 2), the index $\alpha \in \{R,L\}$ denotes the right or left leg of the ladder ($\bar{R}=L$ and $\bar{L}=R$), $\bar{\sigma}=-\sigma$ for $\sigma \in \{\uparrow,\downarrow\}$, and the upper (lower) sign stands for terms with $\alpha=L$ ($\alpha=R$).

The charge-transfer model [Eq. (1)] includes seven orbitals per $Cu_2O_5$ ladder unit cell $i$ (see Fig. 1): two $Cu(3d_{x^2-y^2} \equiv d)$ orbitals on the $R/L$ leg, two $O(2p_y \equiv y)$ orbitals on the $R/L$ leg, two $O(2p_x \equiv x)$ side orbitals on the $R/L$ leg, and one $O(2p_x \equiv b)$ bridge orbital on the rung. Although it seems that the model is quasi-one-dimensional (1D), the density operators $\bar{n}_{i\alpha x\sigma}$ and $\bar{n}_{i\alpha y\sigma}$ stand for the oxygen-hole densities in the neighboring ladders and make it implicitly 2D as the interladder coupling couples the ladders, so the model extends over the entire $Cu_2O_5$ plane.

## III. EFFECTIVE *t-J* HAMILTONIAN

### A. Model and the superexchange

In what follows we will derive the low-energy version of Hamiltonian [Eq. (1)] which is valid in the so-called charge-transfer regime $U>\Delta$, i.e., for the typical values of model [Eq. (1)] parameters: $U \simeq 8t_{pd}$, $\Delta \simeq 3t_{pd}$, and $U_p \simeq 3t_{pd}$, see Ref. 17 and Sec. III E below. The effective *t-J* Hamiltonian consists then of four terms, and may be thus also called *t-J-V* model,

$$H = H_t + H_J + H_{V_1} + H_{V_2}, \tag{5}$$

which are separately derived and discussed below.

We begin with the superexchange term $H_J$ which is the only important term in Eq. (5) at half filling. In this case (i.e., with one hole per copper site), the charge-transfer model [Eq. (1)] can be easily reduced to the low-energy Heisenberg model for spins $S=1/2$ using the perturbation theory to fourth order in $t_{pd}$ (Ref. 18)

TABLE I. Binding energy of the singlet and triplet state formed by the copper hole and a doped hole in one of the three various oxygen states: (i) symmetric plaquette state $|P_{i\alpha\sigma}\rangle$, (ii) antisymmetric plaquette state $|A_{i\alpha\sigma}\rangle$ orthogonal to Eq. (8), and (iii) single oxygen orbital. Here $t_1=t_{pd}^2/\Delta \sim t_{pd}/3$, $t_2=t_{pd}^2/(U-\Delta) \sim t_{pd}/5$, and $t_3=t_1U_p/(\Delta+U_p) \sim t_{pd}/6$ for the typical charge-transfer parameters (Ref. 17).

| | $\lvert P_{i\alpha\sigma}\rangle$ | $\lvert A_{i\alpha\sigma}\rangle$ | Single oxygen |
|---|---|---|---|
| Singlet | $-8(t_1+t_2)+2t_3$ | $-4t_1+2t_3$ | $-2(t_1+t_2)+2t_3$ |
| Triplet | 0 | $-4t_1$ | 0 |

$$H_J = J\sum_{i\alpha}\left(\mathbf{S}_{i\alpha}\cdot\mathbf{S}_{i+1,\alpha} - \frac{1}{4}\tilde{n}_{i\alpha}\tilde{n}_{i+1,\alpha}\right) + J\sum_{i}\left(\mathbf{S}_{iR}\cdot\mathbf{S}_{iL} - \frac{1}{4}\tilde{n}_{iR}\tilde{n}_{iL}\right). \tag{6}$$

Here, tilde in $\tilde{n}_{i\alpha}$ implies that the hole double occupancies are excluded. The superexchange constant contains contributions due to charge excitations on copper sites and on the intermediate oxygen site for a Cu-O-Cu bond, and for finite $U_p$ reads[18]

$$J = \left(\frac{2t_{pd}^2}{\Delta}\right)^2\left\{\frac{1}{U} + \frac{2}{2\Delta+U_p}\right\}. \tag{7}$$

One may wonder whether the geometry of coupled ladders could influence the above result. Indeed, there exists a 90° superexchange process between the holes on two neighboring ladders. However, according to the Goodenough-Kanamori rules[19] such a superexchange process is much weaker than the superexchange generated by charge excitations along the 180° path in the single ladder and can be neglected.

### B. Zhang-Rice singlets for the ladder

When the ladder is away from half filling, the perturbation theory gets complicated. Therefore, following the Zhang and Rice (ZR) construction,[2] we first define a phase-coherent *symmetric plaquette state*[20] $|P_{i\alpha\sigma}\rangle$, which is formed by the four oxygen orbitals surrounding the central copper site $i\alpha$

$$|P_{i\alpha\sigma}\rangle = \frac{1}{2}(\pm x^\dagger_{i\alpha\sigma} \mp b^\dagger_{i\sigma} - y^\dagger_{i-1,\alpha\sigma} + y^\dagger_{i\alpha\sigma})|0\rangle, \tag{8}$$

where the upper (lower) sign stands for $\alpha=L$ ($\alpha=R$). When a hole in this state forms a singlet state with the hole at the central copper site, it has a large negative binding energy of $-8(t_1+t_2)+2t_3$, see caption of Table I for definition of $t_n$ hoppings and for more details. Actually, this binding energy is not only much larger than the individual effective hopping terms (which is on the order of $t_1$ or $t_2$, see Ref. 2) but it is also considerably larger than the binding energy of some other possible bound states, see Table I. Note that finite $U_p$, not considered by Zhang and Rice,[2] results in finite $t_3$ hopping but does not qualitatively change the large binding energy of a symmetric singlet state [Eq. (8)].

The mere problem with the states defined by Eq. (8) is that they are not orthogonal. It can be checked that in the case of the ladder geometry the following superposition of the symmetric plaquette states forms a complete and orthogonal basis for a low-energy Hilbert subspace

$$\phi^\dagger_{l\alpha\sigma}|0\rangle = \frac{1}{N}\sum_{jk} e^{ikl}e^{-ikj}(\alpha_k|P_{j\alpha\sigma}\rangle + \beta_k|P_{j\bar{\alpha}\sigma}\rangle), \tag{9}$$

where $\alpha_k(\beta_k)=2/\sqrt{3-2\cos k}\pm 2/\sqrt{5-2\cos k}$. Then the ZR singlets for the ladder are

$$|\psi_{i\alpha}\rangle = \frac{1}{\sqrt{2}}(\phi^\dagger_{i\alpha\uparrow}d^\dagger_{i\alpha\downarrow} - \phi^\dagger_{i\alpha\downarrow}d^\dagger_{i\alpha\uparrow})|0\rangle. \tag{10}$$

Although the binding energy is slightly reduced after this orthogonalization, the change is not significant: if the energy splitting between the orthogonalized ZR singlets and triplets is defined as $16\chi^2 t_1$ (we consider a simplified case $t_1=t_2$ and $U_p=0$), then $\chi\approx 1$—both in the 1D ($\chi=0.98$) and in the 2D case ($\chi=0.96$), see Ref. 2.

Having shown that the ZR singlets in the single ladder do not differ much from those which arise in the 2D cuprates,[21] we can now safely apply all the arguments used in Ref. 2 to derive the effective hopping of ZR singlets following from finite $t_{pd}$. Thus, we obtain,

$$H_t = -t\sum_{i\alpha\sigma}\{\tilde{d}^\dagger_{i\alpha\sigma}\tilde{d}_{i\bar{\alpha}\sigma} + (\tilde{d}^\dagger_{i\alpha\sigma}\tilde{d}_{i+1,\alpha\sigma} + \text{H.c.})\}, \tag{11}$$

where once again $\tilde{d}_{i\alpha\sigma}=d_{i\alpha\sigma}(1-n_{i\alpha\bar{\sigma}})$ is a fermion operator in the restricted space. While we do not show here the detailed expression for the effective hopping $t$ of ZR singlets, note that it is considerably smaller than $t_{pd}$ ($\sim$50%).[2] Note also that having two ZR singlets at the same site costs energy $4t_2+2t_1$ (if $t_3=0$, see Ref. 2) and therefore we used the tilde operators above to exclude these local configurations of two ZR singlets.

### C. Intraladder repulsion $H_{V_1}$

The Coulomb interaction on oxygen sites $U_p$, neglected in Ref. 2, plays a minor role in the stability of the ZR singlets (see, e.g., finite $t_3$ for finite $U_p$ in Table I), but this issue is more subtle.[22] Actually, due to finite $U_p$ the two neighboring nonorthogonal ZR singlets repel each other when two holes occupy a common oxygen site (see Figs. 2 and 3). Whereas the significance of the interladder repulsion is discussed in the next section, let us concentrate first on the repulsion between the ZR singlets *within a single ladder* (see Fig. 2), and calculate repulsion $\propto U_p$ between two orthogonalized ZR singlets within the ladder $\langle\psi_{s\alpha},\psi_{r\beta}|\mathcal{H}_1|\psi_{h\beta},\psi_{j\alpha}\rangle$. Let us note that the "mixed terms" such as $\langle\psi_{sR},\psi_{rL}|\mathcal{H}_1|\psi_{hL},\psi_{jL}\rangle$, which could *a priori* destroy the ZR singlets, fortunately turn out to be much smaller than the respective binding energy. Using Eq. (10), after a somewhat lengthy but straightforward calculation (for more details see Appendix A), one finds the following values for the intraladder interaction along the leg and the rung

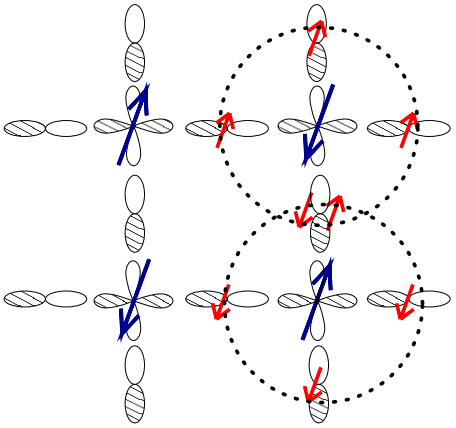

FIG. 2. (Color online) The artist's view of the intraladder repulsion between two neighboring ZR singlets. Large (small) arrows depict the hole spins for +1.0(+0.25) charge—they stand for spins at copper sites and for the spins of doped holes delocalized over oxygen orbitals. Orbital phases are depicted by striped/white areas.

$$\langle\psi_{j\alpha},\psi_{j+1,\alpha}|\mathcal{H}_1|\psi_{j+1,\alpha},\psi_{j\alpha}\rangle = 0.027U_p, \tag{12}$$

$$\langle\psi_{j\alpha},\psi_{j\bar{\alpha}}|\mathcal{H}_1|\psi_{j\bar{\alpha}},\psi_{j\alpha}\rangle = 0.026U_p. \tag{13}$$

We have verified that the interaction between the second-nearest neighbors is $\sim$15 times smaller and can be safely neglected (the longer-range interaction is even smaller, cf. Appendix A).

Hence, one finds that the interaction among the nearest-neighbor ZR singlets is almost isotropic. Thus, we can write the effective Hamiltonian for the repulsion between ZR singlets (as shown in Fig. 2)

$$H_{V_1} = V_1\left(\sum_{i\alpha}\tilde{n}_{i\alpha}\tilde{n}_{i+1,\alpha} + \sum_i \tilde{n}_{iR}\tilde{n}_{iL}\right), \tag{14}$$

where $V_1\simeq 0.027U_p$. Let us note that the ratio $V_1/U_p$ is approximately 14% smaller than the naively estimated nonorthogonal value $1/32=0.03125$. We also checked that dimensionality drives the following trend in the ratios $V_1/U_p$: 0.023, 0.025, 0.027 (considered here), and 0.029, for a single rung, the 1D case, a ladder, and the 2D case, so $V_1/U_p$ increases with the increasing number of neighbors.[22] This follows because in lower dimensions the charge escapes more

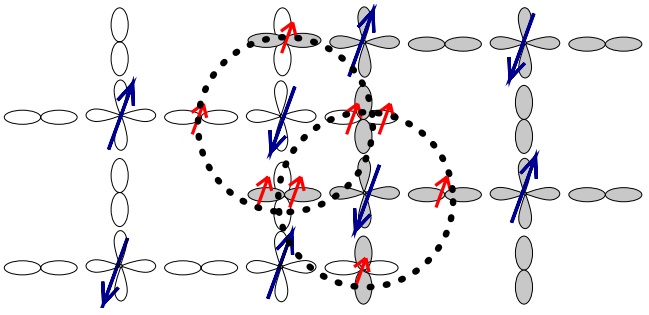

FIG. 3. (Color online) The artist's view of the interladder repulsion between two ZR singlets on two different (white and gray) ladders. Spins are depicted similarly as in Fig. 2.

TABLE II. Adopted values of the parameters of the charge-transfer model [Eq. (1)] from Ref. 17 ($J_H$ from Ref. 14) and the calculated values of the derived $t$-$J$-$V$ model [Eq. (5)] in electron volt.

| Charge-transfer model | | $t$-$J$-$V$ model | |
|---|---|---|---|
| $t_{pd}$ | 1.3 | $t$ | 0.54 |
| $\Delta$ | 3.6 | $J$ | 0.24 |
| $U_p$ | 4.0 | $V_1$ | 0.11 |
| $U$ | 10.5 | $V_2$ | 0.27 |
| $J_H$ | 0.8 | | |

easily from the orbitals $b$ and $y$ (providing the dominating contribution), while in the 2D case *all* the orbitals suffer from the orthogonality problem.

### D. Interladder repulsion $H_{V_2}$

Finally, we calculate the *interladder* repulsion between the ZR singlets due to on-site repulsion $U_p$ in orbitals belonging to two neighboring ladders: $\langle \psi_{s\alpha}, \bar{\psi}_{r+1/2,\beta} | \mathcal{H}_2 | \bar{\psi}_{h+1/2,\beta}, \psi_{j\alpha} \rangle$—a *bar* sign over $\psi$ denotes the singlet formed on the neighboring ladder. Besides, since the neighboring ladder is misaligned by a lattice constant 1/2 with respect to the one considered, we label the ZR singlets on the neighboring ladder by $j+1/2$ (for the copper-copper lattice constant equal to 1). Next, using Eq. (10) one finds after a somewhat tedious but straightforward calculation (for more details see Appendix B) the following value for the interladder interaction between the closest sites belonging to the neighboring ladders (see Fig. 3),

$$\langle \psi_{j\alpha}, \bar{\psi}_{j\pm 1/2,\bar{\alpha}} | \mathcal{H}_2 | \bar{\psi}_{j\pm 1/2,\bar{\alpha}}, \psi_{j\alpha} \rangle = 0.136(1 - 5\eta/2)U_p, \tag{15}$$

while other (neglected) longer-range repulsive terms are at least one order of magnitude smaller, cf. Appendix B. Thus, the repulsion between holes on the neighboring ladders reads

$$H_{V_2} = V_2 \sum_{i\alpha} (\tilde{n}_{i\alpha} \bar{\tilde{n}}_{i+1/2,\bar{\alpha}} + \tilde{n}_{i\alpha} \bar{\tilde{n}}_{i-1/2,\bar{\alpha}}), \tag{16}$$

where $\tilde{n}_{i\alpha}$ operator is related to the ZR singlets as before and $V_2 \simeq 0.136(1-5\eta/2)U_p$. We again neglected all spin-flip terms which are small in comparison with the ZR binding energy and give zero when "sandwiched" in the singlet states. Besides, the numerical prefactor (equal to 0.136) is here slightly enhanced with respect to the expected $1/8 = 0.125$ value (unlike in the intraladder case). This is because a significant fraction of charge escapes from the $b$ and $y$ orbitals to the $x$ orbitals due to the orthogonalization procedure.

### E. Parameters of the effective model

The calculated parameters of the effective $t$-$J$-$V$ model [Eq. (5)] derived above are shown in Table II. This calculation is based on the cuprate charge-transfer model parameters from Ref. 17 (the value of $J_H$ is taken from Ref. 14) which might be considered as the most widely accepted choice of the cuprate parameters, cf. Refs. 21 and 22. Due to the same Cu-O distances in SCCO as in $CuO_2$ planes in, e.g., $La_2CuO_4$, we can adopt these parameters also to the present case.

Let us note that on the one hand, it should be emphasized that the interladder coupling $V_2$ is on the order of $J$ for the realistic parameters[14,17] and therefore *cannot be neglected*. On the other hand, the value of $V_1$ is two and a half times smaller and therefore we suggest that, if necessary, this interaction could be skipped in the first-order calculations.

## IV. ROLE OF THE INTERSITE COULOMB REPULSION $V_{pd}$

One may wonder whether the intersite Coulomb repulsion $V_{pd}$ in the charge-transfer model could alone lead to a significant repulsion (i.e., on the order of the estimated value of $V_2$) between the ZR singlets in the neighboring ladders. This term, which stands for the repulsion between charges situated in the nearest-neighbor copper $3d$ and oxygen $2p$ orbitals, was neglected in Ref. 9 and in the above analysis, cf. Eq. (1). In fact, including this term may, e.g., lead to a significant renormalization of the parameters of the 2D $t$-$J$ model.[23]

Indeed, one finds that the repulsion between a hole in a symmetric state $|\phi_{i\sigma}\rangle$ and a copper hole in state $|d_{j\sigma'}\rangle$ situated on the nearest-neighbor sites in two neighboring ladders is on the order of $(n_{ix\sigma}+n_{iy\sigma})n_{dj\sigma'}V_{pd} \sim 0.5V_{pd}$. Although typically $V_{pd}$ is smaller than $t_{pd}$, e.g., $V_{pd} \sim 1.2$ eV (Ref. 17) or even $V_{pd} \leq 1$ eV,[24] this contribution might still be significant and, in principle, should not be entirely neglected. However, the key observation is that this term leads to roughly equally large energy cost if: (i) *either* the two ZR singlets are situated on the above-mentioned sites $i$ and $j$ and repel each other due to $V_{pd}$ *or* (ii) the two ZR singlets are situated far away from each other on two ladders and (due to $V_{pd}$) merely feel the repulsion with the neighboring copper hole on the neighboring ladder. Hence, including the intersite repulsion $V_{pd}$ increases the total energy of the system but almost does not contribute to the energy difference between the two above situations, measured by the value of the interladder repulsion $V_2$. It is only a small residual repulsion due to the orthogonalization procedure, see Eq. (9), which may change the value of $V_2$ by a small fraction. This has been also confirmed by the results of Ref. 22, where $V_{pd}$ leads indeed to a very small repulsion between holes in the 2D $t$-$J$ model ($\sim 0.05t_{pd}$).

## V. NUMERICAL RESULTS

Now we shall verify whether the derived $t$-$J$-$V$ model in Eq. (5) supports the CDW states observed in SCCO and to understand to what extent the interladder term [Eq. (16)] influences the stability of the CDW state. As a thorough investigation is beyond the scope of this work and left for future studies, we solve the model [Eq. (5)] in the simplest possible way. Thus, we first introduce the Gutzwiller factors, $g_t = (2-2n)/(2-n)$ and $g_J = 4/(2-n)^2$, which renormalize the

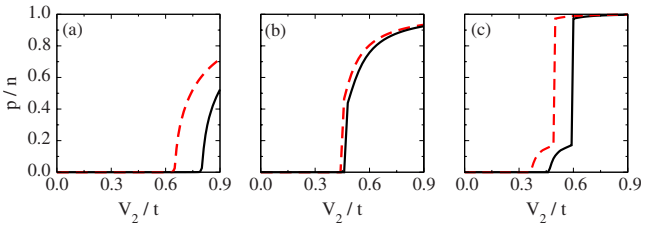


FIG. 4. (Color online) The self-consistently calculated order parameter $p$ for SCCO as obtained from the effective $t$-$J$-$V$ model [Eq. (5)] [see Eq. (17) and text for more details] as a function of the interladder interaction $V_2$ for: (a) filling $n=2/3$ and period $\lambda=3$, (b) $n=3/4$ and $\lambda=4$, (c) $n=4/5$ and $\lambda=5$. Parameters: realistic values (see text) $J=0.4t$ and $V_1=0.2t$ (solid lines), and $J=0$ and $V_1=0$ (dashed lines).

kinetic ($g_t$) and interaction ($g_J$) terms; for their justification see, e.g., Ref. 25. Here $n$ denotes the average number of $d$ holes per site in the effective model [Eq. (5)], i.e., $n=\Sigma_\sigma\langle\bar{n}_{i\alpha\sigma}\rangle$. Second, we use the mean-field approximation for the interaction terms. Next, we diagonalize the effective one-particle Hamiltonian introducing the classical fields

$$\langle d^\dagger_{i\alpha\sigma}d_{i\alpha\sigma}\rangle=\begin{cases} n-p & \text{for } i/\lambda\in\mathbb{Z} \\ n+\dfrac{1}{\lambda-1}p & \text{for } i/\lambda\notin\mathbb{Z}, \end{cases} \tag{17}$$

where $p\leq n$ is the CDW order parameter and $\lambda$ is the CDW period. Furthermore, $\langle\bar{d}^\dagger_{i-1/2,\alpha\sigma}\bar{d}_{i-1/2,\alpha\sigma}\rangle$ are defined as in Eq. (17) but with $i/\lambda$ replaced by $(i+1)/\lambda$ [$(i+2)/\lambda$ for $\lambda=5$]—this assumption minimizes the classical energy cost of the interladder repulsion $V_2$.

In Fig. 4 we show the CDW order parameter $p$ calculated self-consistently as a function of the interladder interaction $V_2$ for the three experimentally interesting doping levels:[9,26] $n=2/3$ which corresponds to $n_h=2-n=4/3$ holes per copper site in charge-transfer model [Eq. (1)], $n=3/4$ corresponding to $n_h=5/4$, and $n=4/5$ corresponding to $n_h=6/5$. The results demonstrate that the interladder interaction plays indeed a crucial role in the stability of the CDW while the intraladder one is rather unimportant.

We have found that the CDW state with period $\lambda=3$ ($\lambda=5$) is stable for $n=2/3$ ($n=4/5$) for the rather realistic values of the parameters $J=0.4t$, $V_1=0.2t$, and $V_2=0.5t-0.9t$. Please note that: (i) we adopted here a somewhat smaller value of $J=0.4t$ which is closer to a typical value for cuprates[27] and (ii) values of $V_2$ exceeding $0.5t$ can be obtained using, for example, the set of parameters suggested in Ref. 24. This finding explains well the experimental results of Ref. 6. Besides, the CDW-ordered state is also stable for period $\lambda=4$ which was not observed.[6] We expect that the stability of the CDW state with this period is a shortcoming of the above-simplified solution which does not capture well the frustration between two possible CDW patterns in the neighboring ladders, which occurs for period $\lambda=4$.[9]

## VI. CONCLUSIONS

In summary, we derived the $t$-$J$ model, which describes the low-energy physics of $Cu_2O_5$ coupled ladders. Apart from the "standard" superexchange $\propto J$ and kinetic-energy terms $\propto t$, the model contains also the repulsion between the nearest-neighbor holes in a ladder $\propto V_1$ and in the two neighboring ladders $\propto V_2$, and hence is also referred to as a $t$-$J$-$V$ model [see Eq. (5)]. We showed that the latter $V_2$ term is roughly two and a half times larger than $V_1$ and (contrary to $V_1$) cannot be skipped—in fact it is crucial to explain the onset of the odd period CDW state in SCCO. We emphasize that this particular extra term is restricted to the copper oxides in which oxygen is coordinated by three copper ions in the same plane. Therefore, it is not present in the $CuO_2$ planes,[12] or in Cu-O chain[13] in copper oxides, but (apart from the discussed SCCO case) could become relevant for the coupled chains of $SrCuO_2$ (provided they are hole doped). Furthermore, it is both a many-body term *and* on the order of $J$, contrary to various corrections to a 1D or 2D $t$-$J$ model.[4,22] Besides, we also verified that the Coulomb intersite interaction $V_{pd}$ alone (not included in the presented derivation) cannot lead to a significant interladder repulsion $V_2$.

The simple mean-field solutions of the $t$-$J$-$V$ model derived here provides evidence in favor of the experimental observations of the onset of the odd CDW state in the ladder planes of the SCCO. This is further supported by the recent density-matrix renormalization-group calculations[27] where a ladder $t$-$J$ model with the interladder coupling $V_2$ (denoted as $V_\perp$ in Ref. 27) was studied: also there the CDW with odd period is stabilized due to the presence of the interladder interaction $V_2$.

Finally, let us note that the other hole-doped ladder compound $La_{1-x}Sr_xCuO_{2.5}$ is also characterized by a large (but different than the one discussed here) interladder coupling.[28] Therefore, we argue that it is currently a challenge for the condensed-matter community to search for a hole-doped ladder compound which could indeed be modeled by the ladder $t$-$J$ Hamiltonian [given by Eqs. (6) and (11), i.e., without additional intersite repulsion terms].

## ACKNOWLEDGMENTS

We thank Alexander Chernyshev for insightful discussions and Maria Daghofer for the critical reading of the manuscript. We acknowledge financial support by the Foundation for Polish Science (FNP) and the Polish Ministry of Science and Education under Project No. N202 068 32/1481. K.W. thanks University of British Columbia for the kind hospitality.

## APPENDIX A: DERIVATION OF THE INTRALADDER REPULSION TERM $\propto V_1$

Here we show how to calculate the repulsion between orthogonalized ZR singlets within the ladder due to the on-site interaction $U_p$ in $\mathcal{H}_1$. Thus, one needs to determine the following matrix elements

$$\langle\psi_{s\alpha},\psi_{r\alpha}|\mathcal{H}_1|\psi_{h\alpha},\psi_{j\alpha}\rangle,\quad \langle\psi_{s\alpha},\psi_{r\bar{\alpha}}|\mathcal{H}_1|\psi_{h\bar{\alpha}},\psi_{j\alpha}\rangle. \tag{A1}$$

Let us note that the mixed terms such as for example $\langle\psi_{sR},\psi_{rL}|\mathcal{H}_1|\psi_{hL},\psi_{jL}\rangle$ vanish in the ZR singlet basis—they could a priori lead to the destruction of the ZR singlets but

fortunately they are much smaller than the respective binding energy.

*Intraladder repulsion along the leg*. First, we calculate the matrix elements of $\mathcal{H}_1$ between the orthogonal plaquette states Eq. (9) along the leg

$$\langle \phi_{s\alpha\sigma}, \phi_{r\alpha\bar{\sigma}} | \mathcal{H}_1 | \phi_{h\alpha\bar{\sigma}}, \phi_{j\alpha\sigma} \rangle = \frac{1}{16} U_p \frac{1}{N^3} \sum_{kqf} e^{ik(h-r)} e^{iq(j-s)} e^{if(r-s)} \times \left\{ \frac{1}{16} (\alpha_k \alpha_q + \beta_k \beta_q - \alpha_k \beta_q - \beta_k \alpha_q)(\alpha_{q-f} \alpha_{k+f} + \beta_{q-f} \beta_{k+f} - \alpha_{q-f} \beta_{k+f} - \beta_{q-f} \alpha_{k+f}) + \left( \sin\frac{k}{2} \sin\frac{q}{2} \sin\frac{q-f}{2} \sin\frac{k+f}{2} + \frac{1}{16} \right) (\alpha_k \alpha_q \alpha_{q-f} \alpha_{k+f} + \beta_k \beta_q \beta_{q-f} \beta_{k+f}) \right\}, \tag{A2}$$

and

$$\langle \phi_{s\alpha\sigma}, \phi_{r\alpha\bar{\sigma}} | \mathcal{H}_1 | \phi_{h\alpha\sigma}, \phi_{j\alpha\bar{\sigma}} \rangle = - \langle \phi_{s\alpha\sigma}, \phi_{r\alpha\bar{\sigma}} | \mathcal{H}_1 | \phi_{h\alpha\bar{\sigma}}, \phi_{j\alpha\sigma} \rangle \tag{A3}$$

while the same spin elements are zero,

$$\langle \phi_{s\alpha\sigma}, \phi_{r\alpha\sigma} | \mathcal{H}_1 | \phi_{h\alpha\sigma}, \phi_{j\alpha\sigma} \rangle = 0. \tag{A4}$$

One can evaluate numerically the above expressions. It occurs that the largest positive element is the nearest-neighbor interaction

$$\langle \phi_{j\alpha\sigma}, \phi_{j+1,\alpha\bar{\sigma}} | \mathcal{H}_1 | \phi_{j+1,\alpha\bar{\sigma}}, \phi_{j\alpha\sigma} \rangle = 0.0544 U_p \tag{A5}$$

while following Eq. (A3) the absolute value of the largest negative element, which corresponds to spin-flip nearest-neighbor interaction, is the same. Furthermore, the second largest element is the next nearest-neighbor interaction and is over 20 times smaller, which means that it can be safely neglected.

Second, we calculate the matrix elements of $\mathcal{H}_1$ between the nearest-neighbor ZR singlets, defined by Eq. (10). This introduces a factor 1/2 to the above estimations of the repulsion between orthogonal plaquette states. It is because there is a 50% probability to have opposite spins on a particular shared oxygen site occupied by two holes from two different ZR singlets. Note that the spin-flip-plaquette terms do not give any contribution to the repulsion between ZR singlets, although they could in principle destabilize the ZR states themselves. Fortunately, this is not possible since the binding energy of the ZR singlets is much larger. Thus altogether, we obtain for the repulsion along the same leg

$$\langle \psi_{j\alpha}, \psi_{j+1,\alpha} | \mathcal{H}_1 | \psi_{j+1,\alpha}, \psi_{j\alpha} \rangle = 0.0272 U_p. \tag{A6}$$

*Intraladder repulsion along the rung*. Following a similar scheme, one can calculate the repulsion between ZR singlets on different legs. One obtains the following matrix elements of $\mathcal{H}_1$ between the orthogonal plaquette states Eq. (9) on different legs

$$\langle \phi_{s\alpha\sigma}, \phi_{r\bar{\alpha}\bar{\sigma}} | \mathcal{H}_1 | \phi_{h\bar{\alpha}\bar{\sigma}}, \phi_{j\alpha\sigma} \rangle = \frac{1}{16} U_p \frac{1}{N^3} \sum_{kqf} e^{ik(h-r)} e^{iq(j-s)} e^{if(r-s)} \times \left\{ \frac{1}{16} (\alpha_k \beta_q + \beta_k \alpha_q - \alpha_k \alpha_q - \beta_k \beta_q)(\alpha_{q-f} \beta_{k+f} + \beta_{q-f} \alpha_{k+f} - \alpha_{q-f} \alpha_{k+f} - \beta_{q-f} \beta_{k+f}) + \left( \sin\frac{k}{2} \sin\frac{q}{2} \sin\frac{q-f}{2} \sin\frac{k+f}{2} + \frac{1}{16} \right) (\alpha_k \beta_q \alpha_{q-f} \beta_{k+f} + \beta_k \alpha_q \beta_{q-f} \alpha_{k+f}) \right\}, \tag{A7}$$

and

$$\langle \phi_{s\alpha\sigma}, \phi_{r\bar{\alpha}\bar{\sigma}} | \mathcal{H}_1 | \phi_{h\bar{\alpha}\sigma}, \phi_{j\alpha\bar{\sigma}} \rangle = - \langle \phi_{s\alpha\sigma}, \phi_{r\bar{\alpha}\bar{\sigma}} | \mathcal{H}_1 | \phi_{h\bar{\alpha}\bar{\sigma}}, \phi_{j\alpha\sigma} \rangle, \tag{A8}$$

and

$$\langle \phi_{s\alpha\sigma}, \phi_{r\bar{\alpha}\sigma} | \mathcal{H}_1 | \phi_{h\bar{\alpha}\sigma}, \phi_{j\alpha\sigma} \rangle = 0. \tag{A9}$$

Evaluating numerically the above expressions one obtains that the largest element is the nearest-neighbor repulsion—this time between the orthogonal plaquette states on the same rung

$$\langle \phi_{j\alpha\sigma}, \phi_{j,\bar{\alpha}\bar{\sigma}} | \mathcal{H}_1 | \phi_{j,\bar{\alpha}\bar{\sigma}}, \phi_{j\alpha\sigma} \rangle = 0.0529 U_p \tag{A10}$$

while the second largest element (the next nearest-neighbor interaction) is over 15 times smaller and can be neglected.

Finally, following the same steps as those leading from Eq. (A5) to Eq. (A6), we obtain the repulsion between the nearest-neighbor ZR singlets [defined by Eq. (10)] along the same rung which is twice reduced

$$\langle \psi_{j\alpha}, \psi_{j,\bar{\alpha}} | \mathcal{H}_1 | \psi_{j,\bar{\alpha}}, \psi_{j\alpha} \rangle = 0.0265 U_p. \tag{A11}$$

## APPENDIX B: DERIVATION OF THE INTERLADDER REPULSION TERM $\propto V_2$

Here the task is to calculate the repulsion between two ZR singlets centered at the neighboring copper positions of two ladders (and thus sharing the same oxygen sites but *not* the $p$ orbitals, see Fig. 3) due to the on-site repulsion on oxygen sites. However, again we will calculate the repulsion between arbitrarily located ZR singlets and only then we will show which elements are negligible. Note that the plaquette states on two ladders are orthogonal to each other although they still have to be orthogonalized for the same ladder (as in Appendix A). Explicitly one needs to calculate the following matrix elements:

$$\langle \psi_{s\alpha}, \bar{\psi}_{r+1/2,\bar{\alpha}} | \mathcal{H}_2 | \bar{\psi}_{h+1/2,\bar{\alpha}}, \psi_{j\alpha} \rangle \tag{B1}$$

and

$$\langle \psi_{s\alpha}, \bar{\psi}_{r+1/2,\alpha} | \mathcal{H}_2 | \bar{\psi}_{h+1/2,\alpha}, \psi_{j\alpha} \rangle. \tag{B2}$$

*Interladder repulsion between plaquettes with the same spin.* We calculate the matrix elements of $\mathcal{H}_2$ between the orthogonal plaquette states Eq. (9) with the same spin but situated on different legs

$$\langle \phi_{r\alpha\sigma}, \bar{\phi}_{s+1/2,\bar{\alpha}\sigma} | \mathcal{H}_2 | \bar{\phi}_{h+1/2,\bar{\alpha}\sigma}, \phi_{j\alpha\sigma} \rangle = \frac{1}{16}(1-3\eta)U_p \frac{1}{N^3} \sum_{kqf} \alpha_k \alpha_q \alpha_{q-f} \alpha_{k+f} \left\{ \frac{1}{4} \sin q \, \sin(q-f) + \frac{1}{4} \sin k \, \sin(k+f) \right\} e^{ik(h-r)} e^{iq(j-s)} e^{if(r-s-1/2)} \tag{B3}$$

while for the same legs we obtain

$$\langle \phi_{r\alpha\sigma}, \bar{\phi}_{s+1/2,\alpha\sigma} | \mathcal{H}_2 | \bar{\phi}_{h+1/2,\alpha\sigma}, \phi_{j\alpha\sigma} \rangle = \frac{1}{16}(1-3\eta)U_p \frac{1}{N^3} \sum_{kqf} \alpha_k \beta_q \alpha_{q-f} \beta_{k+f} \left\{ \frac{1}{4} \sin q \, \sin(q-f) + \frac{1}{4} \sin k \, \sin(k+f) \right\} e^{ik(h-r)} e^{iq(j-s)} e^{if(r-s-1/2)}. \tag{B4}$$

As it might have been expected, it occurs that the biggest term is the repulsion between orthogonal plaquette states with the same spin situated on the closest possible sites in the neighboring ladders (see Fig. 3)

$$\langle \phi_{j\alpha\sigma}, \bar{\phi}_{j\pm 1/2,\bar{\alpha}\sigma} | \mathcal{H}_2 | \bar{\phi}_{j\pm 1/2,\bar{\alpha}\sigma}, \phi_{j\alpha\sigma} \rangle = 0.1355(1-3\eta)U_p, \tag{B5}$$

and all other terms are on the order of $10^{-3}(1-3\eta)U_p$ and can be neglected.

*Interladder repulsion between plaquettes with opposite spin.* A very similar calculation as above but performed for the orthogonal plaquette states Eq. (9) with opposite spins leads to the repulsion between orthogonal plaquette states with opposite spins and situated on the closest possible sites in the neighboring ladders

$$\langle \phi_{j\alpha\sigma}, \bar{\phi}_{j\pm 1/2,\bar{\alpha}\bar{\sigma}} | \mathcal{H}_2 | \bar{\phi}_{j\pm 1/2,\bar{\alpha}\bar{\sigma}}, \phi_{j\alpha\sigma} \rangle = 0.1355(1-2\eta)U_p \tag{B6}$$

while again all other longer-range repulsive terms can be neglected.

Finally, combining Eqs. (B5) and (B6) with the definition of the ZR singlet [Eq. (10)] we obtain the value of the repulsion between the two ZR singlets (cf. similar discussion in Appendix A) on the closest possible sites in the neighboring ladders to be

$$\langle \psi_{j\alpha}, \bar{\psi}_{j\pm 1/2,\bar{\alpha}} | \mathcal{H}_2 | \bar{\psi}_{j\pm 1/2,\bar{\alpha}}, \psi_{j\alpha} \rangle = 0.1355(1-5\eta/2)U_p. \tag{B7}$$


[1] K. A. Chao, J. Spałek, and A. M. Oleś, J. Phys. C **10**, L271 (1977); Phys. Rev. B **18**, 3453 (1978).
[2] F. C. Zhang and T. M. Rice, Phys. Rev. B **37**, 3759 (1988).
[3] E. Dagotto, Rev. Mod. Phys. **66**, 763 (1994).
[4] T. A. Maier, M. Jarrell, T. C. Schulthess, P. R. C. Kent, and J. B. White, Phys. Rev. Lett. **95**, 237001 (2005); M. Ogata and H. Fukuyama, Rep. Prog. Phys. **71**, 036501 (2008); L. Spanu, M. Lugas, F. Becca, and S. Sorella, Phys. Rev. B **77**, 024510 (2008).
[5] E. Dagotto and T. M. Rice, Science **271**, 618 (1996).
[6] A. Rusydi, P. Abbamonte, H. Eisaki, Y. Fujimaki, G. Blumberg, S. Uchida, and G. A. Sawatzky, Phys. Rev. Lett. **97**, 016403 (2006).
[7] E. Dagotto, J. Riera, and D. J. Scalapino, Phys. Rev. B **45**, 5744 (1992).
[8] M. Uehara, T. Nagata, J. Akimitsu, H. Takahashi, N. Môri, and K. Kinoshita, J. Phys. Soc. Jpn. **65**, 2764 (1996).
[9] K. Wohlfeld, A. M. Oleś, and G. A. Sawatzky, Phys. Rev. B **75**, 180501 (2007).
[10] S. R. White, I. Affleck, and D. J. Scalapino, Phys. Rev. B **65**, 165122 (2002).
[11] G. Roux, E. Orignac, S. R. White, and D. Poilblanc, Phys. Rev. B **76**, 195105 (2007).
[12] V. J. Emery, Phys. Rev. Lett. **58**, 2794 (1987); A. M. Oleś, J. Zaanen, and P. Fulde, Physica B & C **148**, 260 (1987); C. M. Varma, S. Schmitt Rink, and E. Abrahams, Solid State Commun. **62**, 681 (1987); J. Dutka and A. M. Oleś, Phys. Rev. B **42**, 105 (1990).
[13] A. M. Oleś and W. Grzelka, Phys. Rev. B **44**, 9531 (1991).
[14] J. B. Grant and A. K. McMahan, Phys. Rev. B **46**, 8440 (1992).
[15] T. F. A. Müller, V. Anisimov, T. M. Rice, I. Dasgupta, and T. Saha-Dasgupta, Phys. Rev. B **57**, R12655 (1998).
[16] K. Wohlfeld, in *Lectures on the Physics of Strongly Correlated Systems XI*, edited by F. Mancini and A. Avella, AIP Conf. Proc. No. 918 (AIP, New York, 2007), p. 337.
[17] M. S. Hybertsen, M. Schlüter, and N. E. Christensen, Phys. Rev. B **39**, 9028 (1989).
[18] J. Zaanen and A. M. Oleś, Phys. Rev. B **37**, 9423 (1988).
[19] J. Kanamori, J. Phys. Chem. Solids **10**, 87 (1959); J. B. Goodenough, *Magnetism and the Chemical Bond* (Interscience, Wiley, New York, 1963).
[20] The term "symmetric" refers here to the $d_{x^2-y^2}$ symmetry.
[21] E. Arrigoni, M. Aichhorn, M. Daghofer, and W. Hanke, New J. Phys. **11**, 055066 (2009).
[22] L. F. Feiner, J. H. Jefferson, and R. Raimondi, Phys. Rev. B **51**, 12797 (1995); **53**, 8751 (1996); R. Raimondi, J. H. Jefferson, and L. F. Feiner, *ibid.* **53**, 8774 (1996).
[23] V. I. Belinicher and A. L. Chernyshev, Phys. Rev. B **49**, 9746 (1994).
[24] H. Eskes, G. A. Sawatzky, and L. F. Feiner, Physica C **160**, 424 (1989).
[25] F. C. Zhang, Phys. Rev. Lett. **90**, 207002 (2003); J. Y. Gan, Y. Chen, Z. B. Su, and F. C. Zhang, *ibid.* **94**, 067005 (2005); M. Raczkowski, M. Capello, D. Poilblanc, R. Frésard, and A. M. Oleś, Phys. Rev. B **76**, 140505 (2007).
[26] A. Rusydi, M. Berciu, P. Abbamonte, S. Smadici, H. Eisaki, Y. Fujimaki, S. Uchida, M. Rübhausen, and G. A. Sawatzky, Phys. Rev. B **75**, 104510 (2007).
[27] J. Almeida, G. Roux, and D. Poilblanc, arXiv:1002.4367 (unpublished).
[28] In $La_{1-x}Sr_xCuO_{2.5}$ the interladder coupling even leads to the antiferromagnetic order for $x=0$, see: S. Matsumoto, Y. Kitaoka, K. Ishida, K. Asayama, Z. Hiroi, N. Kobayashi, and M. Takano, Phys. Rev. B **53**, R11942 (1996).